SCIENCE CHINA
Technological Sciences

•Article•

August 2021 Vol.64 No.8: 1752–1764
https://doi.org/10.1007/s11431-020-1735-9

Near-infrared responsive shape memory hydrogels with programmable and complex shape-morphing

WANG QiLin[1†], ZHU Lin[1†], WEI DanDan[1], SUN Huan[1], TANG Chen[1], LIU Zhao[1], LI Ke[1], YANG Jia[1], QIN Gang[1*], SUN GengZhi[3] & CHEN Qiang[1,2*]

[1] *School of Materials Science and Engineering, Henan Polytechnic University, Jiaozuo 454000, China;*
[2] *Wenzhou Institute, University of Chinese Academy of Sciences, Wenzhou 352001, China;*
[3] *Key Laboratory of Flexible Electronics (KLOFE) & Institute of Advanced Materials (IAM), Nanjing Tech University (NanjingTech), Nanjing 211816, China*

Received August 25, 2020; accepted October 12, 2020; published online July 6, 2021

In this work, semi-crystalline nanocomposite hydrogels (i.e., PAAmA_{11}A/GO gels) were synthesized by micellar copolymerization of acrylamide and *N*-acryloyl-11-aminoundecanoic acid (A_{11}A) in the presence of a large amount of sodium dodecyl sulfonate (SDS) micelles and GO nanosheets. The resulting hydrogels (SMHs) not only demonstrated high strength and high toughness, but also exhibited good shape memory property. Because of near-infrared (NIR) light absorbability of GO nanosheets, shape recovery and shape of PAAmA_{11}A/GO gels could be tuned by NIR irradiation. Moreover, bilayer hydrogels and trilayer hydrogels were also fabricated by the integration of shape-memorized PAAmA_{11}A/GO gel and elastic hydrophobic associated hydrogel (E-gel). Based on the NIR-responsive shape memory property and layered structure, shape deformation of bilayer hydrogels and trilayer hydrogels was rather different from the single PAAmA_{11}A/GO gel. Each kind of gel structure exhibited diverse and complex shapes via programmable NIR irradiation. More importantly, the shape morphing of NIR-SMHs-based hydrogels could mimic the hand and flower and be used as actuators.

shape memory hydrogels, near-infrared responsive, bilayer hydrogels, shape deformation, actuators

Citation: Wang Q L, Lin Z, Wei D D, et al. Near-infrared responsive shape memory hydrogels with programmable and complex shape-morphing. Sci China Tech Sci, 2021, 64: 1752–1764, https://doi.org/10.1007/s11431-020-1735-9

1 Introduction

Shape memory hydrogels (SMHs) are a kind of shape memory polymers (SMPs), which contain a large amount of water in their network structure while maintain their shape memory properties [1,2]. Combination shape memory property with soft-tissue like characteristic, SMHs have been explored to be used in the fields of tissue engineering [3–8], soft actuators [9–13] and smart robots [14–16]. Similar to SMPs, the network structure of SMHs often contains an elastic network and a reversible cross-linking network, in which elastic network trends to maintain the permanent shape of SMHs while reversible cross-linking network can provide the temporary shape via suitable external stimulus and programming process [17,18]. Various reversible interactions served as molecular switches have been utilized to design SMHs, including hydrogen bonds, host-guest interactions, hydrophobic interactions, ionic interactions, dipole-dipole interactions, and crystalline domain [19–24]. Heat, pH, ions, electric field, magnetic field, and near-infrared (NIR) light are often used as the external stimuli to control the shape morphing of SMHs [25–30].

Among various stimuli, NIR light has received great attention because it can locally and programmatically heat the SMHs without contact [31–33]. Many NIR-absorbents, in-

†These authors contributed equally to this work.
*Corresponding authors (email: qingang@hpu.edu.cn; chenqiang@hpu.edu.cn)

cluding gold nanorod, carbon nanotube, polydopamine, polypyrrole, Fe_2O_3 or Fe_3O_4, graphene and graphene oxide (GO) [34–42], have been used to transform the light to heat to tune the shape deformation of thermoresponsive hydrogels. However, the polymer matrix of most of these thermoresponsive hydrogels is poly(*N*-isopropylacrylamide) (PNIPAM). For thermoresponsive gels, e.g., PNIPAM gel, the shape morphing of these gels is mainly caused by volume phase transition. As the temperature is higher than lower critical solution temperature (LCST) of PNIPAM gel, the chain collapse leads to the volume change of PNIPAM gel, which results in the mechanical instability and shape deformation. Many NIR-responsive PNIPAM hydrogels have been reported with controlled shape deformation. For example, Wang and coworkers [43–45] reported a series of NIR-responsive PNIPAM/GO hydrogels, and the complex shape deformations of these hydrogels could be achieved by NIR irradiation. Ma et al. [46] also reported multiresponsive poly(*N*-isopropylacrylamide)/GO/poly(methylacrylic acid) (PNIPAM/GO/PMA) hydrogels, and the resulted gels could exhibit multiresponsive 3D complex deformation triggered by heat, pH, ionic strength and remote-controllable NIR light. Relatively, there are only a few works concerning NIR-responsive SMHs. The shape morphing of SMH is based on shape memory effect. Upon heating, the reversible cross-linking network in SMH is destroyed, and the temporary shape of SMH cannot be maintained. As a result, SMH trends to recover the original shape. Recently, Huang et al. [47,48] had reported NIR-responsive SMHs with double network (DN) structure, and the DN SMHs were formed by physically cross-linked gelatin network and chemically cross-linked polyacrylamide (PAAm) network with GO. Owing to the thermoreversible sol-gel transition of gelatin, the temporary shape of DN SMHs could be rapidly recovered to their original shape after NIR irradiation. Yang et al. [49] also found polydopamine particles (PDAPs) composite poly(vinyl alcohol) (PVA) (PVA/PDAPs) hydrogels exhibited ultrafast NIR-triggered shape memory properties. However, these works are focused on shape memory properties rather than shape-morphing.

Motivated by aforementioned works, herein, we reported novel NIR-SMHs containing GO as NIR-absorbent, which could easily control the shape-recovery and shape deformation via NIR irradiation. Our NIR-SMHs were prepared by *in situ* micellar copolymerization of acrylamide (AAm) and *N*-acryloyl-11-aminoundecanoic acid ($A_{11}A$) in the presence of a large amount of sodium dodecyl sulfonate (SDS) micelles and GO nanosheets. Similar to our previous work, the resulted nanocomposite gels (i.e., $PAAmA_{11}A$/GO SMHs or GO gels) are also semi-crystalline hydrogels, which not only showed high tensile properties, but also exhibited NIR-responsive shape memory properties. Moreover, an elastic hydrophobic associated hydrogel (E-gel) was also prepared, and bilayer and trilayer hydrogels were also fabricated via the lamination of GO gel and E-gel. A systemic shape-morphing study of NIR-SMHs as well as NIR-SMH-based bilayer hydrogels and trilayer hydrogels was investigated. Combination of NIR responsive shape memory property of GO gel and layered structure, programmable and complex shapes could be achieved via local NIR irradiation. More importantly, using NIR irradiation, hydrogel hand, flower and actuator could be designed to mimic or achieve relative functions.

2 Experimental

2.1 Materials

Acrylamide (AAm, 98%) was purchased from Sigma-Aldrich China Inc. 2-hydroxy-4′-(2-hydoxyethoxy)-2-methylpropiophenone (Irgacure 2959) was obtained from TCI China Inc. Sodium dodecyl sulfate (SDS), 11-aminoundecanoic acid, acryloyl chloride, ethyl acetate, tetrahydrofuran (anhydrous), sodium sulfate, petroleum ether and lauryl methacrylate (C12M) were all obtained from Aladdin (shanghai) Inc. $A_{11}A$ was synthesized as our previous work [50]. GO was prepared according to the modified Hummers method [51]. All the reagents are used as received without further purification.

2.2 Synthesis of NIR-responsive SMHs

$PAAmA_{11}A$/GO SMHs were prepared via *in situ* micellar copolymerization. Firstly, GO was ultrasonically dispersed in DI water for 1 h. Then, AAm, $A_{11}A$ and SDS were dissolved in the GO solution at 90°C, forming a solution with the total monomer concentration of 30 wt%, the mole ratio of A11AUA/AAm=20/80, SDS concentration of 20 wt% and various GO concentrations. The homogeneous solution was subsequently degassed with N_2 for 10 min to remove oxygen. Thereafter, APS solution was added into the solution and stirred rapidly for 10 s (APS/monomer=0.01 mol%). The solution was injected into a mold and heated at 60°C for 24 h to sufficiently finish the polymerization. The hydrogels with different GO contents were defined as GO*x* gel, which represents *x* mg/mL of GO. In our present work, the concentrations of GO were 0, 5 and 10 mg/mL, respectively. The E-gel was also prepared by micellar copolymerization but using AAm as hydrophilic monomer, lauryl methacrylate (C12M) as hydrophobic comonomer, Irgacure 2959 as UV-initiator and SDS solution as solvent. However, differently, the mole ratio of C12M/AAm was only 2 mol%, and the concentration of SDS solution was 7% (*w*/*v*), which were much lower than those of $PAAmA_{11}A$/GO SMHs. The photopolymerization for preparation of E-gel was conducted under a UV light (8 W) for 1 h at 365 nm.

2.3 Mechanical tests

For tensile tests, uniaxial tensile was performed on the WSM-10KN tester with a 500 N load cell. During the test, the gel specimens were cut into dumbbell shape with 4 mm in width, 40 mm in length and 1 mm in thickness and stretched with a speed of 100 mm/min at room temperature. The fracture strain (ε_f) was defined as $\varepsilon_f = \Delta l/l_0$ (mm/mm), where Δl is the length change and the l_0 is the original length of the sample, and the fracture stress (σ_f) was given by the force divided by cross-sectional area of the as-prepared gel samples. Young's modulus (E) was calculated from the slope of stress-strain curves between the linear deformations at the small strains. The work of extension (W) was calculated from the area below the stress-strain curves up to the fracture point. For cyclic loading-unloading tests, the samples were firstly loaded to the set extension ratio with the speed of 100 mm/min and then unloaded at the same speed. The extension ratio ($\lambda = l/l_0$) was calculated from the ratio of the deformed length l to the original length l_0. The dissipated energy (U_{hys}) was estimated by the area between loading-unloading curves. For tearing tests, the gel films were cut into the shape of trousers (80 mm in length, 10 mm in width, and 1 mm in thickness) and stretched with one arm fixed while the other arm pulled upward at a speed of 50 mm/min. The tearing energy (T) is defined as the work required tearing a unit area, as estimated by

$$T = 2\,F_{ave}\,/\,w,$$

where F_{ave} is determined as the average force of peak values during steady-state tearing and w is the thickness of the sample.

2.4 Other characterizations

Differential scanning calorimetry (DSC) was carried out on PerkinElmer Diamond DSC to characterize the crystalline property of the GO gel. The as-prepared gel was heated from 30°C to 80°C at a heating rate of 0.5°C/min under nitrogen atmosphere. Raman spectra measurements were performed with Via-Laser microscopic confocal Raman spectroscopy (Renishaw, UK) at an excitation wavelength of 514.5 nm with resolution of 1 cm^{-1}, where the spectral range is 500–4000 cm^{-1}. Rheological measurements were conducted on the MCR302 rheometer equipped with a C-PTD200 temperature control system (Anton Paar China Inc.). The gel sample (diameter of 25 mm and thickness of 1 mm) was firstly heated from 20°C to 60°C, and then cooled from 60°C to 20°C, with a temperature change rate of 2°C/min. The cyclic heating-cooling process was repeated three times to characterize the shape memory properties of the gel. In order to compare the rheological properties of GO gel with E-gel, different test modes were applied. During the test, the sample was firstly tested at a constant temperature of 20°C with the same ω and γ as the above rheological test. Then, the temperature was increased to 60°C at a rate of 2°C/min, and the test was continued with the same frequency and amplitude. This cooling-heating process was repeated five times to compare the viscoelasticity of GO gel with E-gel. The storage modulus G' and loss modulus G'' were recorded as a function of temperature with a fixed strain amplitude $\gamma = 1\%$ and angular frequency $\omega = 10$ rad/s. Silicone oil was laid on the edge of the gel samples to prevent water evaporation. For the NIR-responsive experiments, the gels were directly irradiated with NIR laser (1.6 W, 808 nm, 5 mm × 5 mm spot) for up to 20 s and the temperature was recorded by thermal imager (Seek Thermal). To study the shape morphing of our gels, the gels were firstly deformed via various modes, and then irradiated by NIR laser. The shapes were recorded by a conventional camera.

3 Results and discussion

3.1 Preparation of NIR-SMHs

PAAmA_{11}A/GO gels (i.e., GOx gel) were prepared as our previous work with modification [50]. As shown in Figure 1(a), the nanocomposite gels were synthesized by free radical micellar copolymerization in the presence of a large amount of SDS micelles and GO nanosheets using APS as thermal initiator. Owing to the high concentration of SDS (20% (w/v)), a large amount of A_{11}A hydrophobic monomer could be dissolved in the SDS micelles. Although A_{11}A has only 10 -CH_2- groups on its alkyl chain, it had been identified that the -COOH group at the end of alkyl chain can make the gel crystallize in our previous work [45]. As a result, after polymerization, PAAmA_{11}A/GO gels were semi-crystalline gels, which were dual-physically cross-linked by the crystalline domains and GO nanosheets (Figure 1(b)). The successful incorporation of GO nanosheets could be identified by Raman spectroscopy. It is well known that the G band is the characteristic of graphite-like structure, whereas the D band is associated with the graphene. In Figure S1(a), for the GO0 gel, no relative peaks could be found in the spectrum; however, the D and G peaks could be clearly detected at 1339 and 1605 cm^{-1} in the GO5 gel and GO10 gel, respectively. The presence of crystalline domains in PAAmA_{11}A/GO gels was also certified by DSC. In Figure S1(b), it was found the melt temperature (T_m) of GO10 gel was 46.4°C, which was similar to GO0 gel prepared by UV-initiated micellar copolymerization (45.5°C). The semi-crystalline nature of PAAmA_{11}A/GO gels infers they may also possess shape memory property, which is similar to GO0 gels reported in our previous work. The fixation of gel's temporary shape could be achieved by thermal stimulus or external force based on the crystalline domains. When the gel was heated, the crystalline domains in the gel were melted, and the gel could be fixed

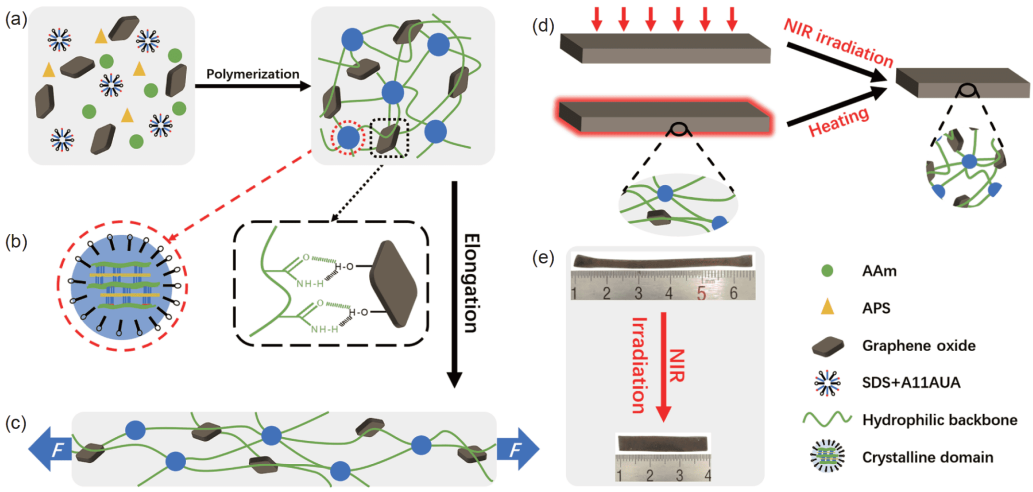

Figure 1 (Color online) Scheme of preparation, network structure and shape memory of PAAmA$_{11}$A/GO gels. (a) Fabrication process of the PAAmA$_{11}$A/GO gels; (b) crystal domain and the interaction between the PAAm chain and the GO nanosheet; (c) stretched structure of PAAmA$_{11}$A/GO gels; (d) shape recovery methods of the PAAmA$_{11}$A/GO gels; (e) shape recovery of PAAmA11A/GO gels under NIR irradiation.

into any shapes because of the cooling-induced recrystallization. If the gel was stretched, the crystalline domains may be partially oriented along with the direction of external force, and shapes could also be fixed (Figure 1(c)). The temporary shape could be recovered to the original shape under heating treatment. Because GO nanosheets in the gels could absorb NIR light and convert it into heat energy due to its NIR-adsorption property, the crystalline domains would be destroyed under NIR irradiation and the gel would trend to recover the original shape on account of the permanent cross-linking of the gel by GO nanosheets (Figure 1(d) and (e)). The NIR-responsive shape memory properties of PAAmA$_{11}$A/GO gels endowed the possibility to locally trigger the shape-morphing of these gels.

3.2 Mechanical properties of NIR-SMHs

The mechanical properties of PAAmA$_{11}$A/GO gels were evaluated by various tests. Distinctly, the tensile properties of the gels could be significantly improved by GO nanosheets (Figure 2(a)). Specifically, as shown in Figure 2(b), the fracture strength (σ_f), elastic modulus (E) and work of extension (W) of GO0 gel were 1.05 MPa, 558 kPa and 7.93 MJ/m^3, respectively. The values of these mechanical parameters were increased as the concentration of GO increased. At GO =10 mg/mL, σ_f, E and W were increased to 1.48 MPa, 2070 kPa and 9.04 MJ/m^3, respectively. In Figure 2(c), the hysteresis loops of PAAmA$_{11}$A/GO gels were increased as the increase of GO concentration, indicating the energy dissipation capacity was also increased. Correspondingly, the dissipated energies at λ=5 for PAAmA$_{11}$A/GO gels at GO= 0, 5 and 10 mg/mL were 0.72, 0.94 and 1.19 kJ/m^3, respectively. From Figure 2(c), it was also found the GO concentration did not affect the residual strain of PAAmA$_{11}$A/GO gels, and all the gels demonstrated the similar and large residual strains, inferring our PAAmA$_{11}$A/GO gels show plastic property after stretching. Moreover, the toughness of PAAmA$_{11}$A/GO gels was also determined by tearing tests. The tearing energies PAAmA$_{11}$A/GO gels were increased from 2694 to 3572 J/m^2 as GO increased from 0 to 10 mg/mL. Compared with our previous work [50], the tearing energies of PAAmA$_{11}$A/GO gels were smaller, which might be caused by the different initiator efficiency under thermal and UV photopolymerization. The results indicate our PAAmA$_{11}$A/GO gels not only demonstrate high strength but also exhibit high toughness, which were attributed to the dual-physically cross-linked network structures. During the deformation, the friction force in crystalline domains and the peeling off PAAm chains from GO nanosheets can dissipate a large amount of energies. Therefore, PAAmA$_{11}$A/GO gels demonstrated high strength, large hysteresis loop and high toughness.

3.3 Rheology tests

Rheological experiments were conducted to evaluate the effect of temperature on the dynamic mechanical properties of PAAmA$_{11}$A/GO gels. As illustrated in Figure 3(a), the storage modulus (G') is always larger than loss modulus (G'') during the heating-cooling cycles, indicating the gel maintained solid-like property. At the 1st heating-cooling cycle, G' was decreased from 2.3×10^5 to 1.0×10^4 Pa as the temperature gradually increased from 20°C to 60°C, and G' was dropped rapidly at ~43°C, which was near to the T_m of GO10 gel (46.4°C). In contrast, G' was increased from 1×10^4 to 3.4×10^5 Pa as cooled from 60°C to 20°C. When heated, the decrease of G' was caused by the melting of crystalline domains, while the increase of G' when cooled was attributed to

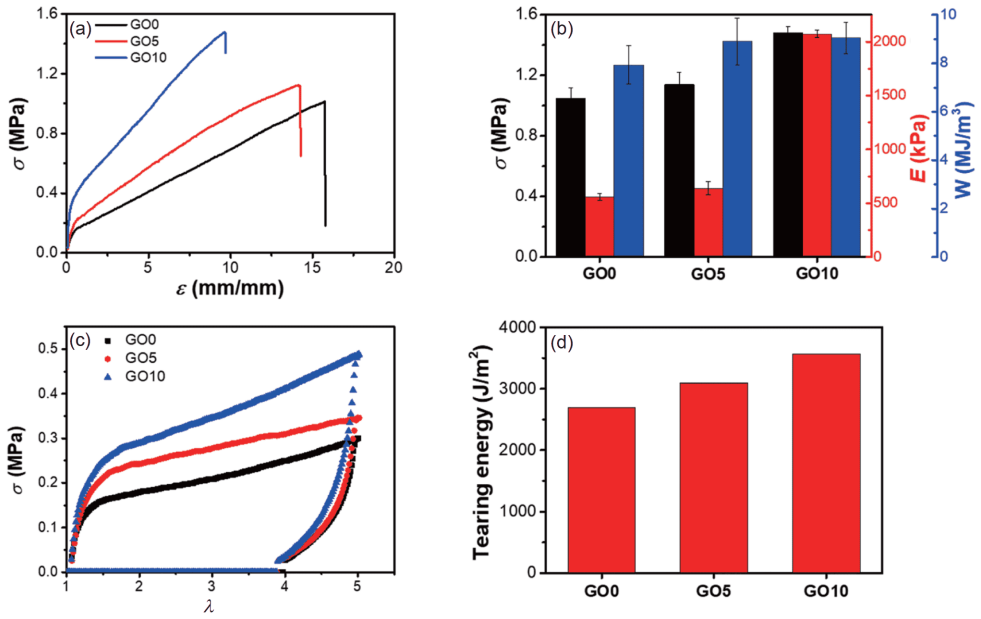

Figure 2 (Color online) Mechanical properties of PAAmA$_{11}$A/GO gels with different GO contents. (a) Stress-strain curves of PAAmA$_{11}$A/GO gels with GO concentration = 0, 5, 10 mg/mL, respectively; (b) effect of GO concentration on the σ_f, E and W of GO PAAmA11A/GO gels; (c) loading-unloading curves of the PAAmA11A/GO gels with various GO concentration; (d) tearing energy of the PAAmA11A/GO gels with various GO concentration.

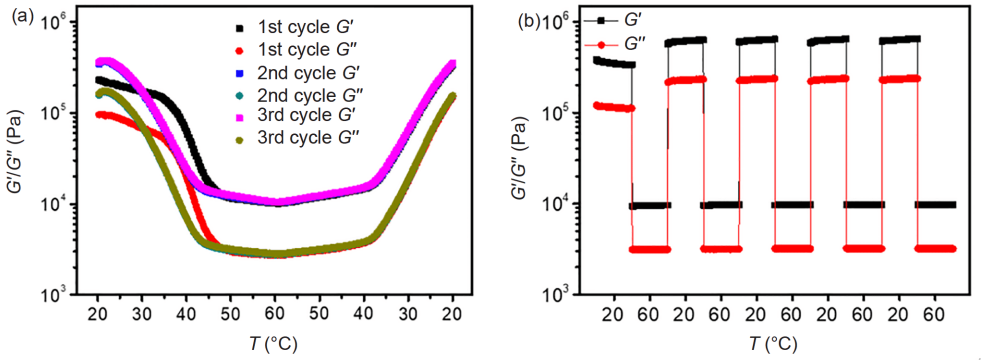

Figure 3 (Color online) Rheology tests of GO10 gel at different test modes. (a) Storage modulus (G') and loss modulus (G'') of GO10 gel for three temperature sweep processes; (b) G' and G'' of GO10 gel at 20°C and 60°C for 5 cycles.

the recrystallization. It should be noted that the 1st heating curve was not overlapped with those of 2nd and 3rd cycles; however, the 1st cooling curve and the cooling curves of 2nd and 3rd heating-cooling cycles were almost overlapped, inferring the recrystallization of A11A side chains in PAAmA$_{11}$A/GO gels during the cooling process was affected by the presence of GO nanosheets cross-linked network. Nevertheless, after the 1st heating-cooling cycle, the network structure of PAAmA$_{11}$A/GO gels could be fully recovered. The changes of G' at 20°C to 60°C after several cycles were illustrated in Figure 3(b). The G' at different temperatures still remained stable after several cycles, and G' at 20°C was ~65 times larger than G' at 20°C, indicating our PAAmA$_{11}$A/GO gels exhibited excellent shape memory property.

3.4 NIR-responsive properties

NIR-responsive properties of PAAmA$_{11}$A/GO gels were also investigated. Figure 4(a) shows the temperature change of the gels with different GO contents as a function of NIR irradiation time. Due to the photothermal effect of GO nanosheets, the temperature of the gels was increased under NIR irradiation. The thermal images of the gels along with NIR irradiation time was illustrated in Figure S2(a). Distinctly, the temperature increased quite fast for all the gels, but the increase rate was also faster for the gels with higher GO content. At the same NIR irradiation time, the temperature of GO10 gel was always higher than that of GO5 gel. Specifically, the temperature of GO10 gel was increased to 82°C after 20 s irradiation, while that of GO5 gel was only

67°C, indicating that there is higher efficiency of NIR energy absorption and transformation at higher concentration of GO nanosheets.

To further investigate the NIR-responsive properties of $PAAmA_{11}A$/GO gels, the gel specimen with different GO contents were fixed into a temporary shape at a right angle of 90° via heating-folding-cooling process, and then the deformed parts were irradiated by NIR irradiation. Owing to the shape memory property of $PAAmA_{11}A$/GO gels, the gels gradually recover the original shape under NIR irradiation-induced heating. The shape recovery process, i.e., recovery angle (θ_r) as a function of NIR irradiation time, was recorded (Figure 4(b)). The curve with a larger slope under the same irradiation time indicates a faster shape recovery rate of the gel. $PAAmA_{11}A$/GO gels demonstrated excellent shape memory properties and could completely recover their original shape. Clearly, the entire recovery process of GO10 gel only required 12 s, while that of GO5 gel took 75 s. Because the shape recovery of semi-crystalline gel requires the melting of crystalline domains in the gel, the faster temperature increase rate of the gel would make the shape recovery process be faster. Therefore, the results are consistent with the results in Figure 4(a). Under NIR irradiation, the temperature of GO10 gel was increased faster, which could lead to faster NIR-induced shape recovery of the gel. Unless otherwise stated, GO10 gel was selected as the model gel for the further shape-morphing investigation.

3.5 Shape-morphing of NIR-responsive SMHs

Base on the NIR-responsive shape memory property of $PAAmA_{11}A$/GO gels, three deformation modes via tuning the deformed position and irradiated area were designed to achieve various complex 3D shapes (Figure 5). In the first mode, as shown in Figure 5(a), the gel underwent an overall deformation through uniaxial stretching, and the gel was fixed into a temporary shape with longer length. After NIR irradiation, the gel rapidly recovered to the original shape. In the second mode, the gel was folded locally and the shape could be recovered after local NIR irradiation (Figure 5(b)). In the third mode, the gel was heated and deformed by external force, and cooled to fix the temporary shape (Figure 5(c)). Then, the gel also recovered to the original shape via NIR irradiation.

Figure 6 demonstrates the shape-morphing of our gels through the three modes. As shown in Figure 6(a), the shape of stretched gel formed by the first mode could be tuned by the NIR irradiated area and direction. If NIR irradiation of stretched gel was local and was along with one direction, the gel was deformed into a "C" shape. However, when the irradiated area was half of the stretched gel, the gel could form a "J" shape. In contrast, if the two irradiated areas were

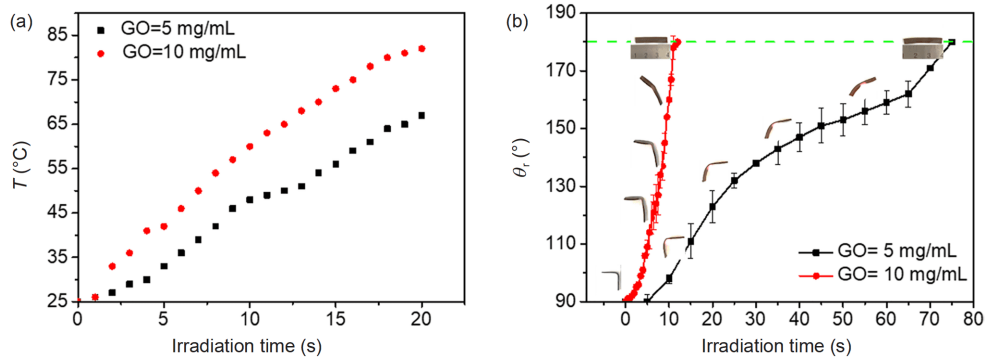

Figure 4 (Color online) NIR-responsive properties of GO gels. (a) Comparison of temperature-irradiation time curves of GO gels under NIR irradiation; (b) comparison of NIR-induced shape memory properties of hydrogels with different GO concentrations.

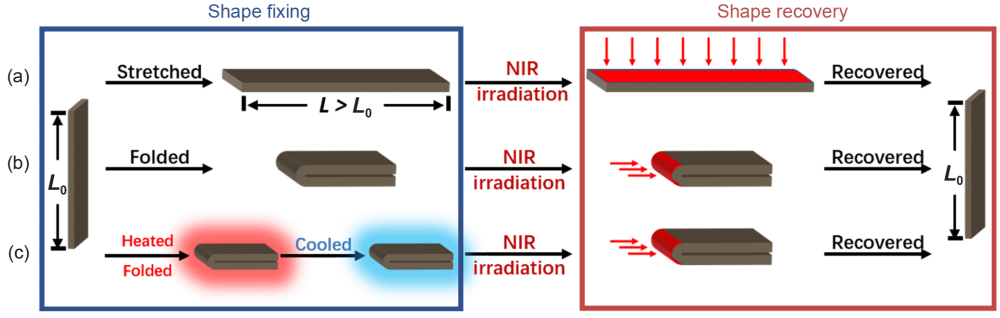

Figure 5 (Color online) Shape fixing and recovery modes of NIR-Responsive SMHs. (a) Uniaxial tensile deformation; (b) folding deformation; (c) heating-cooling deformation.

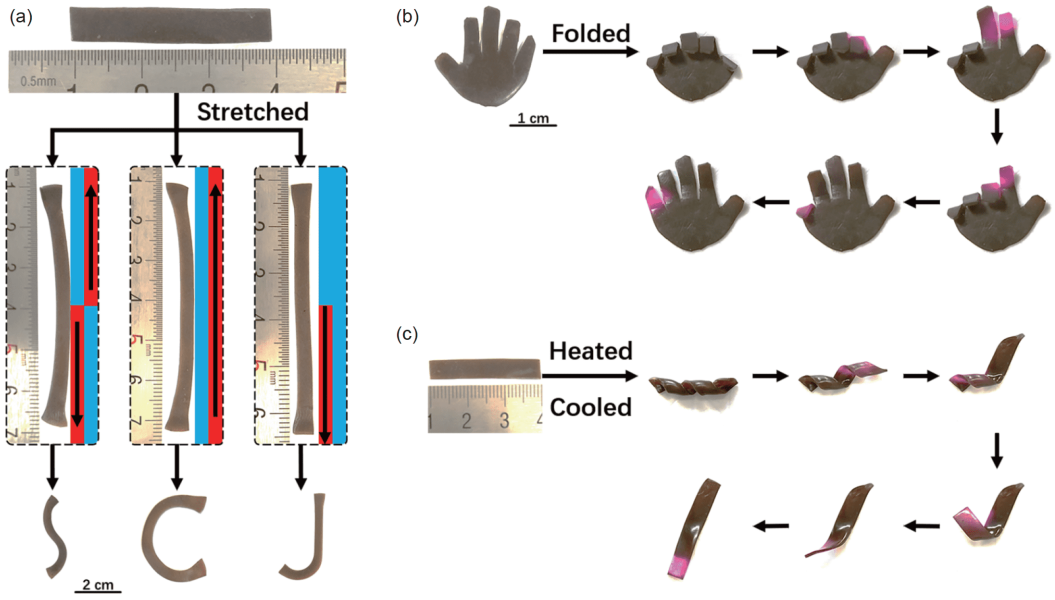

Figure 6 (Color online) NIR-induced shape morphing of PAAmA_{11}A/GO gels. (a) Shape deformation of uniaxially stretched GO gel via various NIR irradiation modes; (b) programmatical shape recovery of folded hydrogel hand; (c) complete recovery of a helical GO gel fixed by heating-cooling mode.

different locations and directions on the stretched gel, the gel became an "S" shape. In Figure 6(b), the gel was cut into a "hand" shape, and all the "fingers" were folded through the second mode. When the folded "fingers" were irradiated by NIR light at the folded area in sequence, the "finger" was orderly spread out and returned to the open "hand" completely. The gel could also be fixed into other 3D shapes through the third mode. In Figure 6(c), the helical gel was irradiated by NIR light along with one direction, and the shape of the gel could be gradually recovered to the 2D rectangle shape. The results indicate the shape-morphing and recovery of our PAAmA_{11}A/GO gels can be simply and programmatically tuned by NIR irradiation.

3.6 NIR-responsive SMHs-based bilayer hydrogels

To further investigate the shape-morphing properties of our PAAmA_{11}A/GO gels, bilayer hydrogels were fabricated, in which PAAmA_{11}A/GO gel (short for GO10 gel) was used as a plastic layer and HPAAm HA gel (i.e., E-gel) was used as an elastic layer. The comparison of GO10 gel and E-gel was found in Figure S2. Distinctly, GO10 gel showed much higher tensile properties than E-gel (Figure S3(a)). The σ_f and E of GO10 gel were 1.48 MPa and 2070 kPa, respectively. However, σ_f and E of E-gel were 0.83 MPa and 14.99 kPa (Figure S3(b)), respectively. Therefore, GO10 gel was 138 times stiffer than E-gel. The G' of E-gel at 20°C was 2×10^4 Pa, which was also much smaller than that of GO10 gel (Figure S3(c)). Moreover, G' of E-gel was not as sensitive as that of GO10 gel when heated. After heating to 60°C, G' of E-gel was only slightly decreased to 1.5×10^4 Pa. In addition, cyclic loading-unloading experiments were also performed as shown in Figure S3(d). Clearly, GO10 gel demonstrated a much larger hysteresis loop than E-gel. Moreover, the former also exhibited much larger residual strain than the latter. Consistently, after stretching, GO10 gel could not recover its original length, but it could be recovered after NIR irradiation, inferring it had plastic property and NIR-responsive shape memory property. In contrast, the length of stretched E-gel could be rapidly recovered with negligible residual strain after the removal of external force, indicating E-gel behaved like an elastic material.

In the presence of work, the bilayer hydrogel was prepared by simply heating the GO gel and E-gel together (Figure 7(a)). Figure 7(a) and (b) illustrated the shape deformation of bilayer hydrogel via overall or local stretching. As mentioned in the experimental section, both GO gel and E-gel were prepared via micellar copolymerization in the presence of surfactant (SDS). GO gel was semi-crystalline gel with a large amount of SDS, which was dual-physically cross-linked by the crystalline domains and GO nanosheets. E-gel was hydrophobically associated hydrogel, and the hydrophobic interactions between alkyl side groups of C12M and SDS micelles are served as physical cross-linkers to cross-link the gel. When the bilayer gels were heated, the crystalline domains in the GO gel were melted, and the hydrophobic interactions in the two gels are similar. The diffusion of polymer chains make the chains be closer, and the rearrangement of hydrophobic interactions leads to the bonding of two gels [52,53].

Because PAAmA_{11}A/GO gel is plastic while E-gel is elastic, the mechanical instability of bilayer gel leads to the

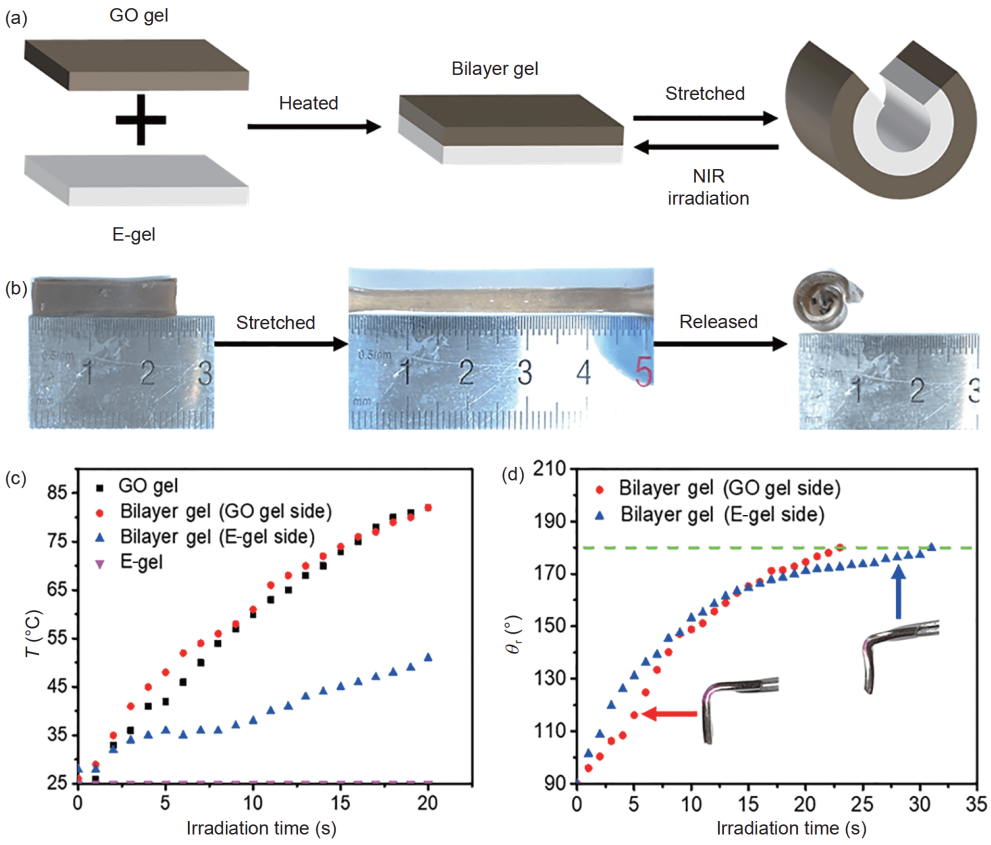

Figure 7 (Color online) Fabrication and NIR-responsive properties of bilayer hydrogels. (a) Illustration of preparation of bilayer hydrogel and its deformation and recovery via uniaxial tensile and NIR irradiation; (b) deformation of bilayer hydrogel under stretching; (c) temperature-irradiation time curves of four irradiated samples; (d) effect of irradiated layer on the shape recovery properties of bilayer hydrogels.

bending or rolling of bilayer gel under stretching. As stretched (i.e., the first mode), the bilayer hydrogel was bent to E-gel side. The center angles of the integrally deformed bilayer gel at various extension ratios (λ) were recorded (Figure S4). The center angle became larger at higher λ, inferring the shape of bilayer hydrogel can be controlled by λ. Different from Figure S4, if the gel was clamped at one end and was stretched, a "6" shape was obtained after the removal of external force (Figure S5(a)). Depending on the direction of external force and patterns of bilayer hydrogel, helical shape and "Ω" shape could be obtained (Figure S5(b) and (c)). If the gel was stretched locally (in the middle of a gel), a "U" shape could be formed (Figure S5(d)). Meanwhile, the bilayer hydrogel could withstand a larger strain of λ= 4 without delamination, indicating that the adhesion between the two gels is quite tight and can bear various complex deformations. The GO gel was NIR-responsive while E-gel was not. The NIR irradiation on different layer of bilayer hydrogel will lead to different temperature responsive behaviors. We irradiated different positions of the bilayer hydrogel with NIR light and recorded the results of their temperature change (Figures 7(c) and S2(b)). The irradiation on GO gel side of bilayer gel was similar to that of GO gel itself, both of them could be heated to 82°C and the temperature *vs.* irradiation time curves were almost overlapped in Figure 7(d). Differently, E-gel is not NIR-responsive gel. After NIR irradiation, no temperature increase could be detected. If NIR irradiated on E-gel side of bilayer gel, the temperature was increased to 52°C at 20 s, which was lower than irradiation on GO gel side. Although E-gel is transparent, due to the blocking of E-gel, the temperature vs. irradiation time curve was totally different (Figure 7(c)). The NIR-responsive behaviors of different layers will also affect the recovery of deformed bilayer hydrogels. As shown in Figure 7(d), one of the bilayer gels was fixed into right angle via the second mode with GO gel layer on the outside and another sample was E-gel layer on the outside. The deformed parts were irradiated with NIR light and the shape recovery process was also recorded with θ_r as a function of NIR irradiation time. The sample with GO gel on the outside required less time to recover its original shape completely (~180°), which was constant with Figure 7(c).

Due to shape memory property of GO gel layer, the temporary shape of bilayer hydrogel can be recovered under NIR irradiation. As shown in Figure S5, the shape recovery of bilayer hydrogels could be controlled by NIR irradiation at

the local area. The "6" shape and "U" shape of bilayer hydrogels could rapidly recover to the original 2D rectangle shape. The recovery of helical shape and "Ω" shape hydrogels was programmable. To further illustrate the programmable shape recovery of bilayer hydrogel, mimic hand and flower were prepared by stretching bilayer hydrogels (Figure 8(a) and (b)). The fingers of the bilayer hydrogel hand were stretched separately, making the hand curl inwards into a fist. Under NIR irradiation, the fingers were programmatically and individually recovered to their original shape, and the palm was opened. The curled fingers in Figure 8(a) were similar to the folded fingers in Figure 6(b). However, considering the structure of human hand, the curled deformation in Figure 8(a) was obviously closer to the actual palm opening process. Similarly, we designed a flower-shaped bilayer hydrogel, whose petals were independent of each other. When the closed petals were irradiated by NIR light separately, the petals are sequentially opened. As shown in Figure 8(c), if the bilayer hydrogel sample was stretched locally at the line position instead of overall stretching, 2D rectangle bilayer hydrogel could form a 3D square-like shape. Based on the precise control properties of NIR light, only the deformed parts were irradiated in sequence, the 3D square-like bilayer gel could programmatically recover to its original 2D rectangle shape. Similarly, a gel box was prepared, and we found the box could be programmatically opened via the irradiation of NIR light at the edges of box. The results indicate the shape-morphing of bilayer hydrogels

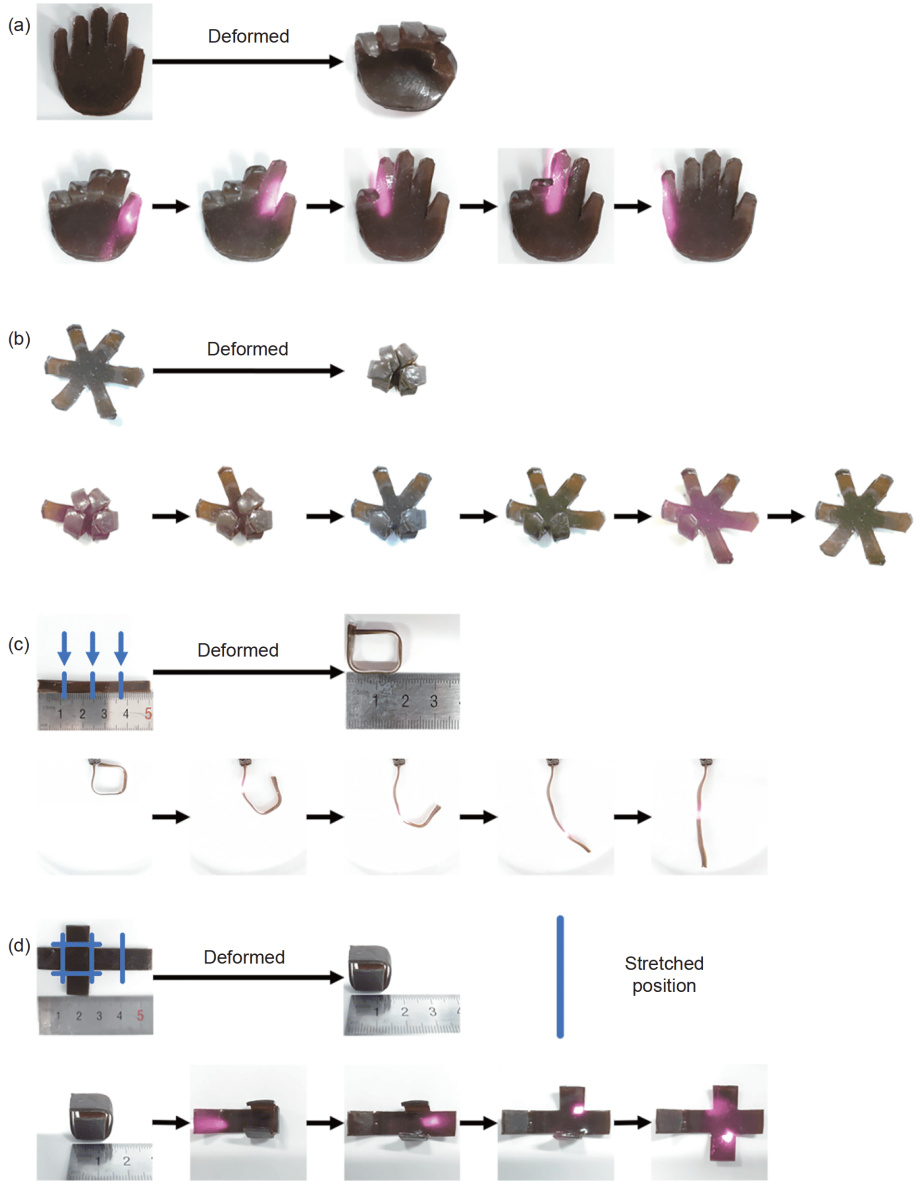

Figure 8 (Color online) Programmatically shape morphing of deformed bilayer hydrogel via NIR irradiation. (a) An opening bilayer hydrogel "hand" and (b) an opening bilayer hydrogel flower prepared via overall deformation; (c) unfolding of a bilayer hydrogel rectangular and (d) opening of a bilayer hydrogel "box" prepared by local deformation.

prepared via the combination of plastic GO gel and elastic E-gel could be easily tuned by overall or local stretching, while the recovered shape of bilayer hydrogels could be programmatically controlled by NIR-irradiation.

3.7 NIR-responsive SMHs-based trilayer hydrogels

Similar to bilayer hydrogels, trilayer hydrogels were also prepared via heating induced adhesion between two GO gels and an E-gel. However, different from bilayer hydrogels, when trilayer hydrogels were stretched, the gels were only elongated but not bent or rolled, i.e., 2D trilayer hydrogels were just formed 2D shapes if stretched (Figure 9(a)). During stretching, all the layers were deformed. After the removal of external force, although the inner E-gel trended to recover its original length, the recovery was restrained by the outer two GO gels. Therefore, the whole trilayer hydrogel could be fixed into an elongated temporary shape without bending. When one of the GO gel layers for elongated trilayer gel was locally irradiated by NIR light, the irradiated area would recover to its original length, and the whole gel would locally bend to the irradiated side (Figure 9(b)). In order to understand the mechanism, we recorded the temperature changes on both sides of the trilayer gel when one of the GO gels was irradiated (Figure 9(c) and (d)). The temperature increase of the irradiated area was consistent with the results in Figure 7(c) and (d), while the temperature of unirradiated GO gel layer was only 38°C after 20 s irradiation of other GO layer, which was lower than T_m of GO10 gel (46.4°C). The difference in temperature of the two GO layers was attributed to the blocking effect of internal E-gel layer. Consequently, the NIR irradiation of GO gel layer for a short time could only cause the shape deformation of the irradiated GO gel layer, while the unirradiated GO gel layer maintained the temporary shape.

Based on the unique deformation and NIR-responsive property, the shape-morphing of trilayer hydrogel could be controlled by NIR irradiation. As shown in Figure 9(d), if the trilayer gel sheet (permanent shape) was stretched in the direction of length, the trilayer gel would be also lengthened in the same direction to form a temporary shape. If the lengthened trilayer gels were NIR irradiated on the single side via different modes, various shapes could be achieved (Figure 9(e)). The trilayer gel would be rolled up if irradiated from the bottom to the top. If irradiated at a 45° angle (the angle is between irradiation direct and the stretching direct), the trilayer gel would form a helical shape. If irradiated at two different local points, the trilayer gel could come into a "U" shape. Both the sides of trilayer gel possess NIR-responsive shape-memory property, and the shapes of trilayer gels can also be controlled by the irradiation of both sides with various modes (Figure 9(f)). If half the trilayer gel was irradiated from the middle to the top while the other half the trilayer gel was irradiated from the middle to the bottom at another side, an "S" shape was achieved. If the trilayer gel was irradiated alternately at different sides and points, the gel would be folded at irradiated points with the angle from 76.82° to 91.29°, depending on the irradiation time. If irradiated alternately at different sides while at the same points, the trilayer gel would alternately bend to the irradiation side with an angle of ~100°. The shape-morphing of trilayer gels could also be tuned via the stretching direction. As shown in Figure 9(g), if the trilayer gel was stretched in the direction of width and was irradiated parallel to the stretching direction on one side, the gel was deformed into a "caterpillar" like shape. If the trilayer gel was biaxially stretched and was also biaxially irradiated, a gel sheet with vertical and horizontal ravines could be obtained (Figure 9(h)). The results indicate various complex shapes could be got via programmatical and local NIR irradiation though the trilayer gels could only form simple temporary shape under stretching.

Based on the alternate bending behavior under NIR irradiation, a trilayer hydrogel flower could mimic the closing and opening of the petals (Figure 10(a)). A cross stitch was made from the trilayer hydrogel, and each arm was stretched. If the arms were irradiated on the top layer in sequence, the trilayer hydrogel flower would be closed, and then the petals would be opened if irradiated on the bottom layer. It should be noted that the hydrogel flower in Figure 10(a) was totally different from that of in Figure 8(b). In Figure 8(b), the close of bilayer hydrogel flower was attributed to external force but not the NIR irradiation. However, in Figure 10(a), the trilayer hydrogel flower not only closed the petals but also opened the petals under NIR irradiation. Moreover, trilayer hydrogel actuator was also fabricated to grab the cargo and release it at another position (Figure 10(b)). The stretched trilayer hydrogel was used as the two arms of the actuator. When the inside area of one of the arms was irradiated by NIR light, the gel was bent inward and the object was grabbed. The object could be lifted up and be moved to the destination. When the object reached the destination, the cargo could be released via irradiating the outside of the same arm (i.e., the arm was bent outwards). In addition, biaxially stretched trilayer hydrogel could be used to record information. As shown in Figure 10(c), the distress signal of "SOS" was remotely and non-contactably written on the gel by NIR irradiation.

4 Conclusion

In summary, novel, tough and NIR-responsive SMHs were synthesized by a facile method using GO nanosheets as NIR-absorbent. The resulted SMHs exhibited high strength (σ_f = 1.48 MPa), high toughness (T = 3572 J/m^2) and good shape memory property. Under NIR irradiation, the optimal GO gel

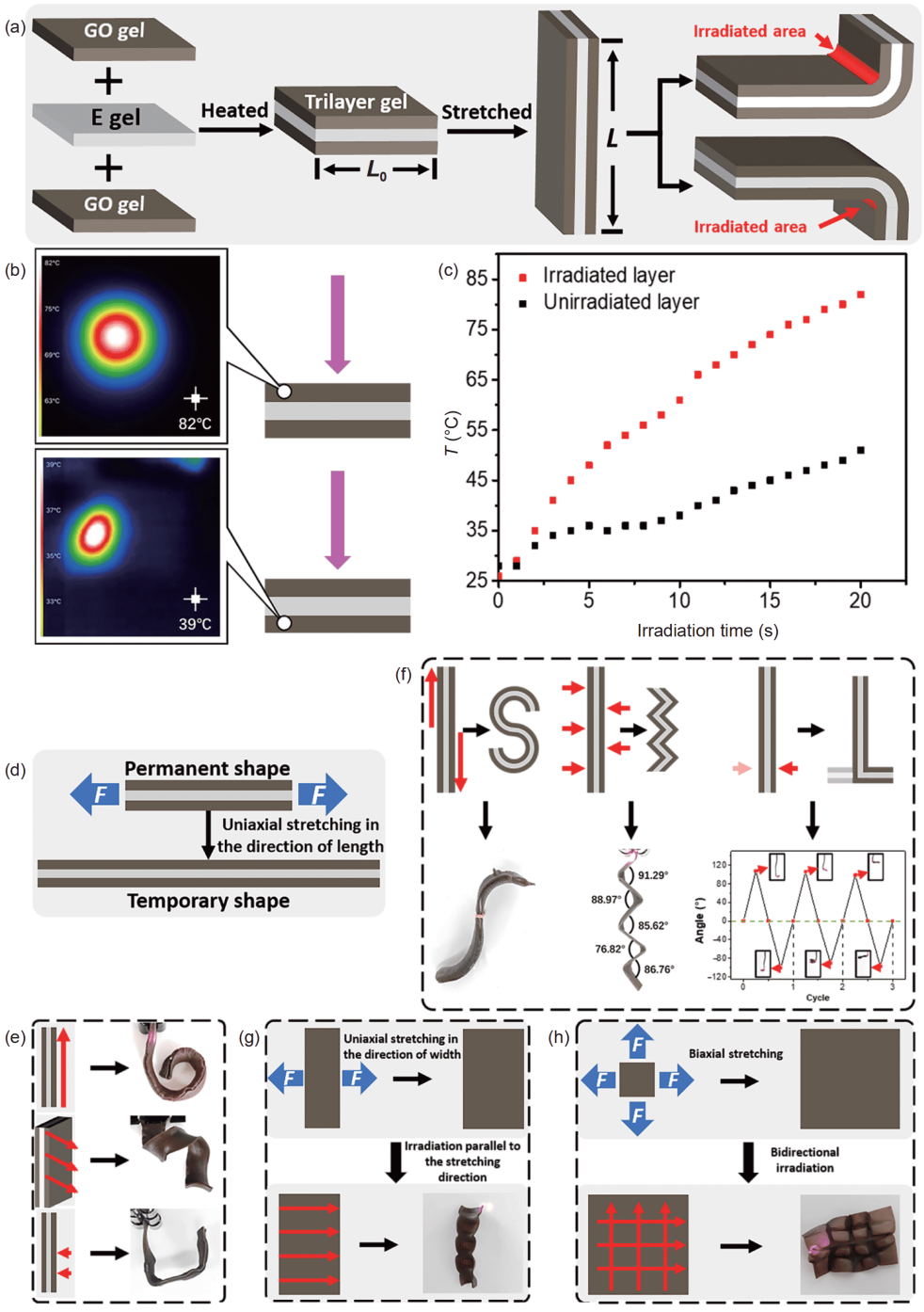

Figure 9 (Color online) Fabrication and shape morphing of trilayer hydrogels under different NIR irradiation modes. (a) Preparation of trilayer hydrogel and deformation of trilayer hydrogel under uniaxial stretching; (b) thermal images of trilayer hydrogel irradiated at the same position for 20 s but recorded at two sides; (c) temperature-irradiation time curves of two sides as NIR irradiated at the same position; (d) under uniaxial stretching in the direction of length, original trilayer hydrogel (permanent shape) was fixed into a temporary shape; (e) shape deformation of uniaxially stretched trilayer hydrogels as NIR irradiated on one side; (f) shape deformation of uniaxially stretched trilayer hydrogels as NIR irradiated on both sides; (g) shape deformation of uniaxially stretched trilayer hydrogel (in the direction of width) as NIR parallelly irradiated along the stretched direction on one side; (h) shape deformation of biaxially stretched trilayer hydrogel as NIR biaxially irradiated on one side.

exhibited rapid temperature increase (82°C for 20 s) and shape recovery. Moreover, NIR-responsive SMH-based bilayer hydrogels and trilayer hydrogels were also fabricated, and a systemic shape-morphing study of NIR-SMHs as well as bilayer hydrogels and trilayer hydrogels was performed. Under local NIR irradiation, deformed NIR-SMHs, bilayer hydrogels and trilayer hydrogels exhibited different while interesting shape morphing behaviors. Various complex

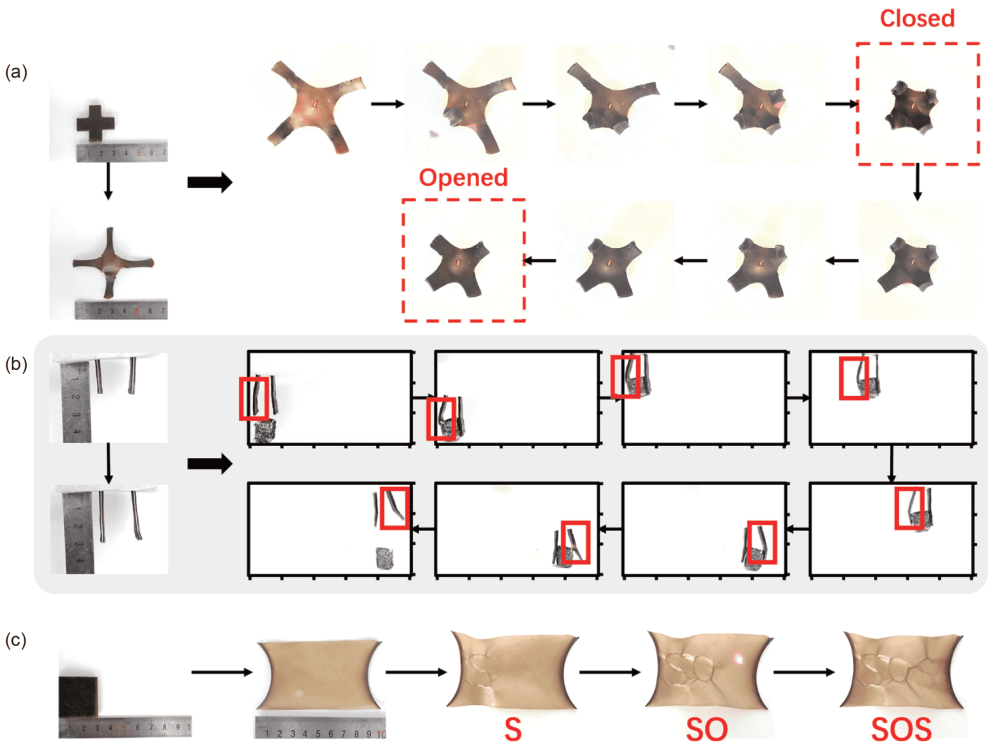

Figure 10 (Color online) Trilayer hydrogel actuators. (a) Closure and reopening of trilayer hydrogel flower; (b) lifting and releasing objects via NIR irradiated on both sides at the same position; (c) writing "SOS" on the surface of biaxially stretched trilayer hydrogel.

shapes could be obtained via programmable NIR irradiation. The shape morphing of NIR-SMHs-based hydrogels could mimic the hand, flower and be used as actuators. This work provides new insights for shape deformation of NIR-SMHs.

This work was supported by the National Natural Science Foundation of China (Grant No. 21504022), the China Postdoctoral Science Foundation (Grant Nos. 2018M642745 and 2020M672179), the Program for Innovative Research Team (in Science and Technology) in the University of Henan Province (Grant No. 19IRTSTHN027), and the Young Backbone Teachers Program of Henan Polytechnic University (Grant No. 2017XQG-06).

Supporting Information

The supporting information is available online at tech.scichina.com and link.springer.com. The supporting materials are published as submitted, without typesetting or editing. The responsibility for scientific accuracy and content remains entirely with the authors.

1 Li T, Li Y, Wang X, et al. Thermally and near-infrared light-induced shape memory polymers capable of healing mechanical damage and fatigued shape memory function. ACS Appl Mater Interfaces, 2019, 11: 9470–9477
2 Fan W, Shan C, Guo H, et al. Dual-gradient enabled ultrafast biomimetic snapping of hydrogel materials. Sci Adv, 2019, 5: eaav7174
3 Yan B, Boyer J C, Habault D, et al. Near infrared light triggered release of biomacromolecules from hydrogels loaded with upconversion nanoparticles. J Am Chem Soc, 2012, 134: 16558–16561
4 Li W, Wang J, Ren J, et al. 3D graphene oxide-polymer hydrogel: near-infrared light-triggered active scaffold for reversible cell capture and on-demand release. Adv Mater, 2013, 25: 6737–6743
5 Zhang E, Wang T, Zhao L, et al. Fast self-healing of graphene oxide-hectorite clay-poly(*N*,*N*-dimethylacrylamide) hybrid hydrogels realized by near-infrared irradiation. ACS Appl Mater Interfaces, 2014, 6: 22855–22861
6 Obiweluozor F O, GhavamiNejad A, Maharjan B, et al. A mussel inspired self-expandable tubular hydrogel with shape memory under NIR for potential biomedical applications. J Mater Chem B, 2017, 5: 5373–5379
7 Wang H B, Li H F, Wu Y H, et al. A high strength, anti-fouling, self-healable, and thermoplastic supramolecular polymer hydrogel with low fibrotic response. Sci China Tech Sci, 2019, 62: 569–577
8 Li Y J, Zhang F H, Liu Y J, et al. 4D printed shape memory polymers and their structures for biomedical applications. Sci China Tech Sci, 2020, 63: 545–560
9 Habault D, Zhang H, Zhao Y. Light-triggered self-healing and shape-memory polymers. Chem Soc Rev, 2013, 42: 7244–7256
10 Wang E, Desai M S, Lee S W. Light-controlled graphene-elastin composite hydrogel actuators. Nano Lett, 2013, 13: 2826–2830
11 Lei Z, Zhou Y, Wu P. Simultaneous exfoliation and functionalization of $MoSe_2$ nanosheets to prepare "smart" nanocomposite hydrogels with tunable dual stimuli-responsive behavior. Small, 2016, 12: 3112–3118
12 Chen Z, Cao R, Ye S, et al. Graphene oxide/poly(*N*-isopropylacrylamide) hybrid film-based near-infrared light-driven bilayer actuators with shape memory effect. Sens Actuat B-Chem, 2018, 255: 2971–2978
13 Hao X P, Xu Z, Li C Y, et al. Kirigami-design-enabled hydrogel multimorphs with application as a multistate switch. Adv Mater, 2020, 32: 2000781
14 Shi K, Liu Z, Wei Y Y, et al. Near-infrared light-responsive poly(*N*-isopropylacrylamide)/graphene oxide nanocomposite hydrogels with ultrahigh tensibility. ACS Appl Mater Interfaces, 2015, 7: 27289–27298
15 Zhang J, Du P, Xu D, et al. Near-infrared responsive MoS_2/poly(*N*-isopropylacrylamide) hydrogels for remote light-controlled micro-

valves. Ind Eng Chem Res, 2016, 55: 4526–4531
16 Zhang C L, Cao F H, Wang J L, et al. Highly stimuli-responsive Au nanorods/poly(*N*-isopropylacrylamide) (PNIPAM) composite hydrogel for smart switch. ACS Appl Mater Interfaces, 2017, 9: 24857–24863
17 Shang J, Le X, Zhang J, et al. Trends in polymeric shape memory hydrogels and hydrogel actuators. Polym Chem, 2019, 10: 1036–1055
18 Ma S Q, Zhang Y P, Wang M, et al. Recent progress in 4D printing of stimuli-responsive polymeric materials. Sci China Tech Sci, 2020, 63: 532–544
19 Xu B, Zhang Y, Liu W. Hydrogen-bonding toughened hydrogels and emerging CO_2-responsive shape memory effect. Macromol Rapid Commun, 2015, 36: 1585–1591
20 Han Y, Bai T, Liu Y, et al. Zinc ion uniquely induced triple shape memory effect of dipole-dipole reinforced ultra-high strength hydrogels. Macromol Rapid Commun, 2012, 33: 225–231
21 Bilici C, Okay O. Shape memory hydrogels via micellar copolymerization of acrylic acid and *n*-octadecyl acrylate in aqueous media. Macromolecules, 2013, 46: 3125–3131
22 Zhao Z, Zhuo S, Fang R, et al. Dual-programmable shape-morphing and self-healing organohydrogels through orthogonal supramolecular heteronetworks. Adv Mater, 2018, 30: 1804435
23 Han X J, Dong Z Q, Fan M M, et al. pH-induced shape-memory polymers. Macromol Rapid Commun, 2012, 33: 1055–1060
24 Liu K, Zhang Y, Cao H, et al. Programmable reversible shape transformation of hydrogels based on transient structural anisotropy. Adv Mater, 2020, 32: 2001693
25 Wei S, Lu W, Le X, et al. Bioinspired synergistic fluorescence-color-switchable polymeric hydrogel actuators. Angew Chem Int Ed, 2019, 58: 16243–16251
26 Liu S, Gao G, Xiao Y, et al. Tough and responsive oppositely charged nanocomposite hydrogels for use as bilayer actuators assembled through interfacial electrostatic attraction. J Mater Chem B, 2016, 4: 3239–3246
27 He X, Sun Y, Wu J, et al. Dual-stimulus bilayer hydrogel actuators with rapid, reversible, bidirectional bending behaviors. J Mater Chem C, 2019, 7: 4970–4980
28 Du X, Cui H, Xu T, et al. Reconfiguration, camouflage, and color-shifting for bioinspired adaptive hydrogel-based millirobots. Adv Funct Mater, 2020, 30: 1909202
29 Zhang Z, Chen Z, Wang Y, et al. Bioinspired bilayer structural color hydrogel actuator with multienvironment responsiveness and survivability. Small Methods, 2019, 3: 1900519
30 Xiao S, Yang Y, Zhong M, et al. Salt-responsive bilayer hydrogels with pseudo-double-network structure actuated by polyelectrolyte and antipolyelectrolyte effects. ACS Appl Mater Interfaces, 2017, 9: 20843–20851
31 Acik M, Lee G, Mattevi C, et al. Unusual infrared-absorption mechanism in thermally reduced graphene oxide. Nat Mater, 2010, 9: 840–845
32 Ma C, Lu W, Yang X, et al. Bioinspired anisotropic hydrogel actuators with on-off switchable and color-tunable fluorescence behaviors. Adv Funct Mater, 2018, 28: 1704568
33 Wang Z J, Li C Y, Zhao X Y, et al. Thermo- and photo-responsive composite hydrogels with programmed deformations. J Mater Chem B, 2019, 7: 1674–1678
34 Lee E, Lee H, Yoo S I, et al. Photothermally triggered fast responding hydrogels incorporating a hydrophobic moiety for light-controlled microvalves. ACS Appl Mater Interfaces, 2014, 6: 16949–16955
35 Deng Z, Guo Y, Zhao X, et al. Multifunctional stimuli-responsive hydrogels with self-healing, high conductivity, and rapid recovery through host-guest interactions. Chem Mater, 2018, 30: 1729–1742
36 Han L, Zhang Y, Lu X, et al. Polydopamine nanoparticles modulating stimuli-responsive PNIPAM hydrogels with cell/tissue adhesiveness. ACS Appl Mater Interfaces, 2016, 8: 29088–29100
37 Hauser A W, Evans A A, Na J H, et al. Photothermally reprogrammable buckling of nanocomposite gel sheets. Angew Chem Int Ed, 2015, 54: 5434–5437
38 Shiotani A, Mori T, Niidome T, et al. Stable incorporation of gold nanorods into *N*-isopropylacrylamide hydrogels and their rapid shrinkage induced by near-infrared laser irradiation. Langmuir, 2007, 23: 4012–4018
39 Wu H, Sheng D, Liu X, et al. NIR induced self-healing polyurethane/polypyrrole nanocomposites. Polymer, 2020, 189: 122181
40 Zhang X, Pint C L, Lee M H, et al. Optically- and thermally-responsive programmable materials based on carbon nanotube-hydrogel polymer composites. Nano Lett, 2011, 11: 3239–3244
41 Zhu C H, Lu Y, Peng J, et al. Photothermally sensitive poly(*N*-isopropylacrylamide)/graphene oxide nanocomposite hydrogels as remote light-controlled liquid microvalves. Adv Funct Mater, 2012, 22: 4017–4022
42 Dai C F, Du C, Xue Y, et al. Photodirected morphing structures of nanocomposite shape memory hydrogel with high stiffness and toughness. ACS Appl Mater Interfaces, 2019, 11: 43631–43640
43 Peng X, Liu T, Jiao C, et al. Complex shape deformations of homogeneous poly(*N*-isopropylacrylamide)/graphene oxide hydrogels programmed by local NIR irradiation. J Mater Chem B, 2017, 5: 7997–8003
44 Peng X, Jiao C, Zhao Y, et al. Thermoresponsive deformable actuators prepared by local electrochemical reduction of poly(*N*-isopropylacrylamide)/graphene oxide hydrogels. ACS Appl Nano Mater, 2018, 1: 1522–1530
45 Peng X, Liu T, Shang C, et al. Mechanically strong Janus poly(*N*-isopropylacrylamide)/graphene oxide hydrogels as thermo-responsive soft robots. Chin J Polym Sci, 2017, 35: 1268–1275
46 Ma C, Le X, Tang X, et al. A multiresponsive anisotropic hydrogel with macroscopic 3D complex deformations. Adv Funct Mater, 2016, 26: 8670–8676
47 Huang J, Zhao L, Wang T, et al. NIR-triggered rapid shape memory PAM-GO-gelatin hydrogels with high mechanical strength. ACS Appl Mater Interfaces, 2016, 8: 12384–12392
48 Zhang E, Wang T, Hong W, et al. Infrared-driving actuation based on bilayer graphene oxide-poly(*N*-isopropylacrylamide) nanocomposite hydrogels. J Mater Chem A, 2014, 2: 15633–15639
49 Yang L, Wang Z, Fei G, et al. Polydopamine particles reinforced poly(vinyl alcohol) hydrogel with NIR light triggered shape memory and self-healing capability. Macromol Rapid Commun, 2017, 38: 1700421
50 Wei D, Yang J, Zhu L, et al. Semicrystalline hydrophobically associated hydrogels with integrated high performances. ACS Appl Mater Interfaces, 2018, 10: 2946–2956
51 Yan X, Yang J, Chen F, et al. Mechanical properties of gelatin/polyacrylamide/graphene oxide nanocomposite double-network hydrogels. Compos Sci Tech, 2018, 163: 81–88
52 Jiang G, Liu C, Liu X, et al. Construction and properties of hydrophobic association hydrogels with high mechanical strength and reforming capability. Macromol Mater Eng, 2009, 294: 815–820
53 Gulyuz U, Okay O. Self-healing poly(acrylic acid) hydrogels with shape memory behavior of high mechanical strength. Macromolecules, 2014, 47: 6889–6899